Advances in Social Science, Education and Humanities Research, volume 528
Proceedings of the 7th International Conference on Research, Implementation, and Education of Mathematics and Sciences (ICRIEMS 2020)

Structure Interpretation Using Gravity Spectral Analysis and Derivative Method in Grindulu Fault, Pacitan, East Java

Mustika N Yusvinda[1],* Shania W Puspitasari[1], Nadia M P Wafi[1], Khafidh N Aziz[1], Denny Darmawan[1], Laila Katriani[1], Novita T Handayani[2] and Nugroho B Wibowo[3]

[1] *Department of Physics Education, Universitas Negeri Yogyakarta, Indonesia*
[2] *Department of Physics, Universitas Gadjah Mada, Indonesia*
[3] *Meteorological, Climatological, and Geophysics Agency: BMKG, Yogyakarta, Indonesia*
[*]*Corresponding author. Email: mustikanovananda.2017@student.uny.ac.id*

ABSTRACT
The Grindulu Fault is a one of the fault that lies alongside the Pacitan Regency, East Java. This fault is a land geological structure that is potential to be the source of earthquake disaster. The structure interpretation is carried out using gravity data by performing spectrum analysis and derivative methods to get a better understanding of the Grindulu Fault. We used gravity data from GGMplus. Spectrum analysis is performed by using Fourier transform to the bouguer anomaly. This Spectral Analysis generates a depth estimation of Grindulu Fault Zone anomaly source. Analysis of derivative methods provides information regarding the location of the fault anomaly source and information about the type of fault. Based on the result of spectral analysis, Grindulu Fault anomaly source is estimated to be at the upper limit of 160 meters and the lower limit up to 2897 meters. The Grindulu fault is interpreted to be segmented into at least 7 parts which is consisted of normal and reverse fault segmentations.

Keywords: *Grindulu Fault, GGMplus, Spectral Analysis, Derivative Method.*

1. INTRODUCTION

Fault interpretation has become one of the main research in earthquake risk disaster management. In Indonesia, especially Java and Sumatera Island, the active subduction movement implies on active deformation through subsurface structure such as fold and fault [1]. Fault movements can cause a major destructive event in surface when earthquake occurs. Many incidents have proven that continental fault is one of a weak zone that became favorite pathways of the earthquake wave propagation, or even became the source of that eartquake itself. With thousands of faults exists in Java, study about fault is very important and should be considered in spatial planning of our society [2].

Regionally, Pacitan has several faults across its area based on geological map. The structures developed are mostly complicated as they were contolled by various main stresses of different tectonic regime. Pacitan is located in transition zone between cretacous subduction trend dominated and tertiary subduction trend dominated [3]. This makes the structures formed in Pacitan have several dominant trends and develop into different types of faults. The trends and types of the faults that developed is the NE-SW sinistral strike slip fault, N-S dextral and sinistral strike slip fault, and NW-SE dextral strike slip fault [4].

The Grindulu Fault as the main object of this research, is one of the active sinistral strike faults with NE-SW trend. The movement of this fault is detected by some earthquake events that occured before and have hiposenter lied on this fault area [5]. This fault was formed due to deformation process in the Middle Miocene and had reactivation during Plio-leistosen Period. Grindulu Fault passes through several lithology formations, which are Arjosari, Mandalika, and Jaten [6].

We used gravity data derived from GGMPlus gravity data set, which is a common method to understanding the subsurface structure. Gravity data can

provide information about density variation caused by lithology and structure. This gravity data is studied using spectrum analysis to determine the approximate depth of the anomaly and derivative analysis to determine the fault boundaries and the type of fault.

2. METHODOLOGY

The research is conducted by processing GGMPlus Gravity Data Model which is reconstructed by satellite data, EGM2008, and short scale topographic effect [7]. We used Free Air Anomaly/Gravity Disturbance. We also used the elevation data derived from Digital Elevation Model (DEM) SRTM. These input data is processed into gravity bouguer anomaly. This anomaly is then used to performed further analysis, which are spectral and derivative analysis.

2.1. Bouguer Anomaly

Bouguer Anomaly is generated from gravity disturbance which is corrected by topographic reduction consists of simple bouguer correction (Bullard A) and terrain correction (Bullard C). This correction is function of elevation and topographic density. To calculate the surrounding effect, we carried out terrain correction. This correction is calculated by measuring the effect of various topography around observed point. The calculation of terrain correction is the used to reduce the bouguer anomaly by using formula [8]:

$$g_c = g_b + T_c = (g_d - 2\pi\gamma\rho h) + T_c \quad (1)$$

With g_c is complete bouguer anomaly (mGal), and T_c is the calculated terrain correction (mGal), g_b is simple bouguer anomaly (mGal), g_d is gravity disturbance data (mGal), γ is the universal gravitational constant, ρ is density as we used general continental plate density (g/cc), and h is the elevation of the observed point. The complete bouguer is then used as the input of more advance processing which are spectral analysis and derivative method analysis.

2.2. Spectral Analysis

Spectral analysis is performed to determine the depth estimation of the anomaly source that controls the subsurface density variation. This analysis was performed per-incision data on each coordinate axis. We used 8 incisions for x-axis (vertical incision) and 6 incisions for y-axis (horizontal incision). The spectral analysis is the performed by applying Fourier transform of bouguer anomaly in every incision. This transforming process algorithm is derived from gravitational potential observed in a horizontal plane. To obtain a direct relationship between amplitude, wave number, and the depth estimation of anomalies source, a logarithmic calculation is performed on the amplitude spectrum to produce a linear equation as follows [9]

$$\ln A = (z - z_0)|k| \quad (2)$$

This equation used to determine the depth of anomaly source in every incision. This graph plot is then divided into 3 parts of linear trendline to generate the gradient value (interpreted as the depth of regional anomaly, local anomaly, and noise).

2.3. Derivative Method

Derivative mothod was performed to clarify the anomaly lineament. It could help to determine the position of the anomaly and interpret the type of density discontinuity anomaly which is interpreted as a fault. We performed two types of derivative methods, which are First Horizontal Derivative (FHD) and Second Vertical Derivative (SVD). FHD of gravity anomaly is a gradient value from one point to another horizontally with a certain distance.

FHD method analysis is performed by derivatng the vertical component of the gravitational field on each x-axis and y-axis. The total quadrat of derivative of these two component results is then rooted to generate the total first horizontal derivative. Based on the value of the gravitational field in a horizontal plane, the horizontal derivative is easier to apply using a finite derivative method with discrite calculation [10].

SVD method analysis is performed by orde-2 derivating the vertical component of the gravitational field on z-axis. This method could enhance the near surface shallow effect of the deeper anomalies. Second vertical derivative is obtained through the computation of second horizontal derivatives of the potential field following Laplace equation [10].

$$\frac{\partial^2 g_z}{\partial z^2} = -\left(\frac{\partial^2 g_z}{\partial x^2} + \frac{\partial^2 g_z}{\partial y^2}\right) \quad (3)$$

SVD Method analyisis would give information in a form of graphic plot which has maximum and minimum values. The subtraction of absolute value of the maximum SVD (Peak) with absolute value of the minimum SVD (Through) will correlated with the degree and the type of the discontinuity plane/fault. A normal fault will generate positive value of the subtraction result, while reverse fault will generate negative value. When the value of subtraction approaches 0, the plane of discontinuity will aso approaches dip 90^0 [11].

3. RESULT AND DISCUSSION

The value of gravity anomaly in the study area ranges from 92 mGal to 118 mGal (Figure 1).

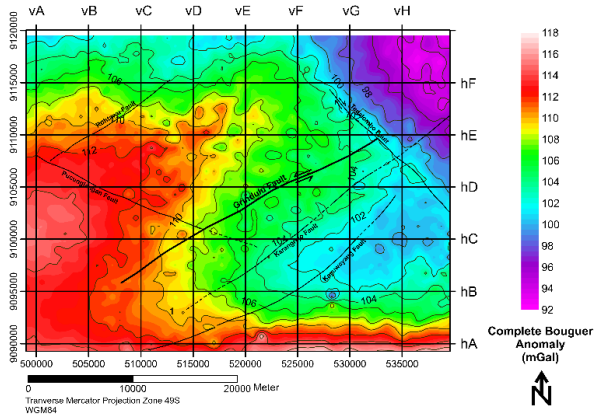

Figure 1. Complete Bouguer Anomaly with Incisions of Spectral Analysis to estimating depth anomaly.

Spectral analysis is performed per horizontal and vertical incision according to the following Figure 1. The Fourier transformation process and logarithmic calculations on the bouguer anomaly slice on each incision resulted in sampling data with variables x and y. The sampling data is then plotted to form a logarithmic graph. To interpret the depth of the source anomaly, 3 gradients were determined for the graph. The largest gradient is interpreted as the depth of the regional anomaly, the smaller gradient is interpreted as a local anomaly, and the smallest gradient is interpreted as noise. Examples of the graphic plots and analysis on the vertical incision vE and the horizontal incision hD are shown in figure 2 and figure 3.

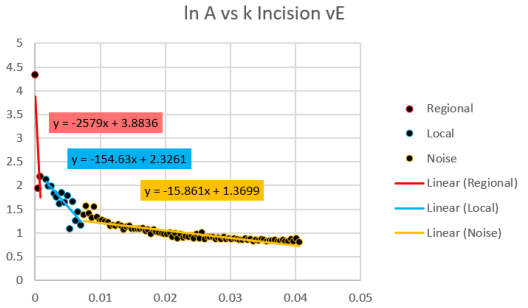

Figure 2. Graphic ln Amplitude (n) vs wavenumber (k) Incision vE. The data shows 3 gradient trendlines interpreted as the depth of anomaly.

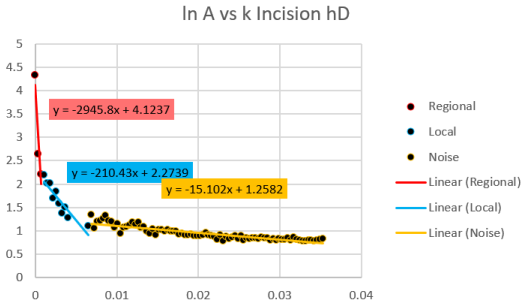

Figure 3. Graphic ln Amplitude (n) vs wavenumber (k) Incision hD. The data shows 3 gradient trendlines interpreted as the depth of anomaly.

The graphic plot above is 2 of the 14 incisions which has been analysed. Each graph generates regional, local, and noise anomaly source depth data, as well as wave number cut-off (| k |) and ln amplitude (N).

Table 1. Depth estimation based on spectral analysis of vertical incision and horizontal incision anomaly

Incision	Regional (m)	Local (m)	Incision	Regional (m)	**Local (m)**
vA	2545.4	100.74	hA	3603.30	**106.52**
vB	2662.4	121.74	hB	2882.70	**105.55**
vC	2460.7	142.45	hC	2691.10	**141.54**
vD	2361.8	130.05	hD	2945.80	**210.43**
vE	2579.0	184.31	hE	3069.30	**184.31**
vF	2406.6	160.45	hF	2524.90	**108.89**
vG	2067.8	178.43			
vH	2072.7	138.20			
Avg Fault Area	2375.2	159.14		2897.23	**160.46**
Avg Total	**2394.6**	**144.55**		**2952.85**	**142.87**

Regional anomalies, which can be caused by the presence of subduction and deep intrusion in the study area are estimated to be at a variation in the depth of the upper limit of 2394 to 2953 meters. This depth varies according to the bouguer anomaly response (Figure 1) where the depth of this anomaly will vary from shallow depth correlates with high anomaly and deep depth correlates with low anomaly. In the zone where the fault passes, the upper limit of the regional anomaly is in the depth range of 2275 to 2897 meters. This value is still in the range of regional anomalies throughout the study area so that the anomaly from the Grindulu Fault is estimated not to be deeper than this range.

Local anomalies, where the response of Grindulu Fault is estimated to be at this depth, has an upper boundary depth variation of 143 to 145 meters in all of research area. In the only Grindulu fault zone, upper boundary depth is estimated on the depth 160 meters. From this, we get an estimation of Grindulu fault anomaly depth which has the upper limit of 160 meters to the lower limit of 2275 to 2897 meters.

The interpretation result of the fault existence are marked with a dashed line in red in Figures 4, 5, and 6.

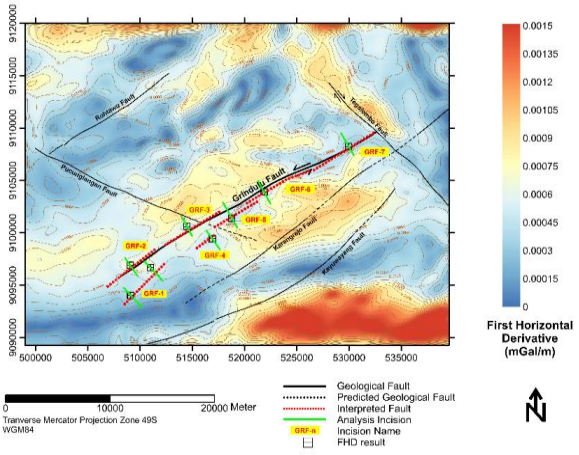

Figure 4. First Horizontal Derivative Map of regional bouguer anomaly in the area of study with interpreted fault.

The results of the FHD processing are shown in Figure 4. Overall, this FHD map shows the dominance of the anomaly with the NE-SW trend. The anomaly in the FHD result is marked by the maximum or minimum value. In the Grindulu fault zone, it can be observed that the FHD anomaly is a minimum value which is presented as blue color. Although the minimum anomaly is not as low as in the northern and southern parts of the fault, the presence of negative anomalies in the Grindulu fault is an enough evident considering that this fault is a sinistral shear fault that does not have much vertical throw apart from the minor structures.

The SVD map shown in Figure 5 shows clearer lineaments.

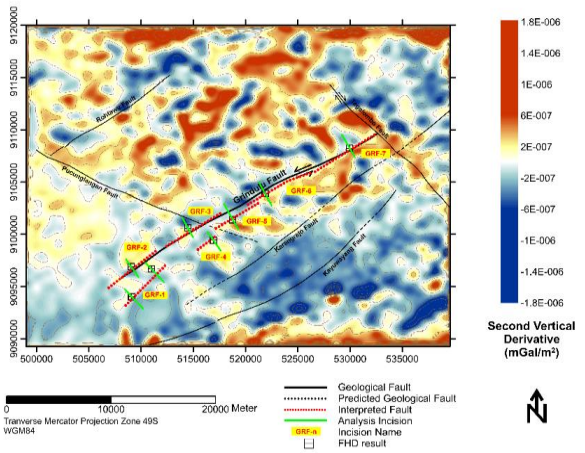

Figure 5. Second Vertical Derivative Map of regional bouguer anomaly in the area of study with interpreted fault

Anomalies location in SVD is marked by 0 value or the white area on the map. Along the trend of Grindulu fault, there are several SVD anomaly lineaments which are segmented. From the FHD and SVD maps, we interpreted at least 7 Grindulu Fault Segmentations, which is shown by the dashed red line. Each of these segments is named as in the yellow label. Furthermore, derivative analysis will be carried out for each of these fault segmentations. The incisions for derivative analysis are shown on the green colored line.

The results of fault segmentation interpretations above are then brought back to the bouguer anomaly in Figure 6.

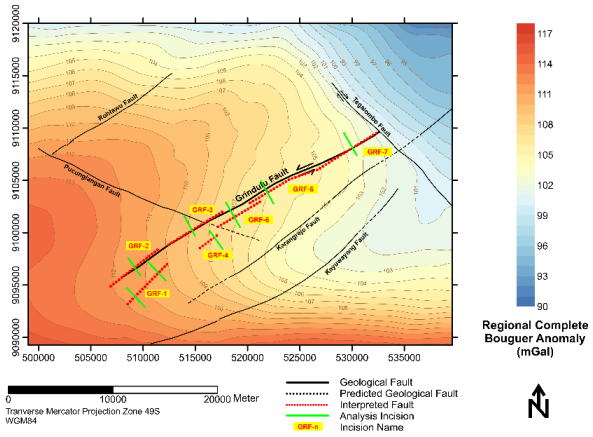

Figure 6. Interpreted fault in Bouguer Anomaly. The trend of anomaly is dominantly controlled by deep anomaly source.

These Grindulu fault segments are located in middle to high anomaly shown by white to red color, and the bouguer anomaly is also elongated into NE-SW orientation as well as the Grindulu Fault.

The incisions for derivative analysis shown by the green line were used to excise the bouguer, FHD, and SVD anomalies. The overlay graphic plot of that three

data are shown for example in Figure 7 and Figure 8. Figure 7 and Figure 8 are 2 samples of the 8 incisions made in the 7 fault segments.

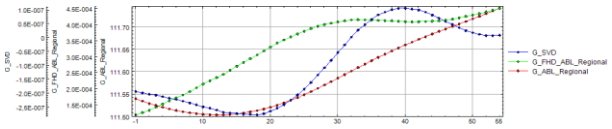

Figure 7. Fault Interpretation using graphic analysis in Incision GRF1. This graphic shows the correlation between bouguer anomaly, first horizontal derivative (FHD) result, and second horizontal derivative (SVD) result. Anomaly edge is shown by yellow line, as it has maximum/minimum FHD and zero SVD.

Figure 7 shows a graphic analysis of the western GFR1 section. The incision is shows 2 peaks of FHD and 2 values of 0 SVD. To consider which one should be use as response of the fault segment GRF1, the addition of 1 adjacent incision (GRF1b) was made. From the results of the GRF1b analysis, GRF1a is interpreted by selecting the first maximum FHD data and the first 0 SVD value shown on the yellow line in Figure 7.

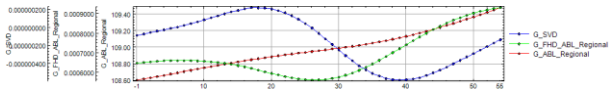

Figure 8. Fault Interpretation using graphic analysis in Incision GRF3. This graphic shows the correlation between bouguer anomaly, first horizontal derivative (FHD) result, and second horizontal derivative (SVD) result. Anomaly edge is shown by yellow line, as it has maximum/minimum FHD and zero SVD.

Figure 8 shows a graphic analysis of the GRF3 incision. In this data, the position of the source anomaly is clearly visible at the minimum value of FHD and value of 0 SVD. From the graph analysis, information can be generated in the form of (i) XY coordinates of location where the FHD value is maximum or minimum, (ii) the minimum SVD value (through) and (iii) the maximum SVD value (peak). The SVD peak value is then reduced by the SVD through value. The results are then used to identify the type of interpreted fault segmentations.

From the results, it can be observed the results of the analysis in the form of the type of fault in each segment of the Grindulu Fault. The reverse fault is interpreted exist as the GRF1, GRF3, GRF4, and GRF6 fault segments. Meanwhile, GRF2, GRF5, and GRF7 fault segments are interpreted as normal faults.

The existence of various fault types of Grindulu Fault segmentations indicates that the deformation that occurs around the fault is complex. Although the Grindulu Fault is a strike-slip fault with minor vertical throw, the bend and step over between segments are allow the construction of reverse and normal fault segments consequently. Research on geodynamics and fault movement mechanisms is needed to get a better understanding of the Grindulu Fault.

4. CONCLUSION

From the results of spectrum analysis, it can be concluded that the depth of the anomaly source from the Grindulu Fault is estimated to be at the upper limit of 160 meters and the lower limit up to 2897 meters. Through the analysis of the FHD and SVD maps, the interpretation of the Grindulu fault is segmented into at least 7 parts. SVD analysis on these seven fault segmentations shows that those segmentations have different types of fault. GRF 1, GRF3, GRF4, and GRF6 are interpreted as reverse fault, while GRF2, GRF5, and GRF7 are interpreted as normal fault.

AUTHORS' CONTRIBUTIONS

MNY, SWP, NMPW, and KNA conceived and designed the analysis. MNY, KNA, and NTH collected data and analyzed it. MNY, SWP, NMPW, KNA, and NTH drafted the manuscript. DD, LK, and NBW contributed in improvement in the manuscript in terms of conceptualization, and final drafting of the manuscript.

ACKNOWLEDGMENTS

We would like to thank to "Fakultas Matematika dan Ilmu Pengetahuan Alam Universitas Negeri Yogyakarta" for the Hibah PKM 70 Judul. We are grateful to Western Australian Geodesy Group, Curtin University for the gravity data used in this study. We would like to thank the anonymous reviewers for important suggestions and comments.

REFERENCES

[1] C C Plummer, D H Carlson, and L Hammersley, Physical Geology, New York: McGraw-Hill Education, 2011.

[2] Y S Kim and D J Sanderson, Earthquake and Fault Propagation, Displacement and Damage Zones, UK: Nova Science Publisher, Inc, 2008, pp. 99-117.

[3] Fahrudin, A S Hidayatillah and M J Maulana, Tectonic Relationships and Structural Development between Arjosari, Pacitan, East Java and Tawangmangu, Karanganyar, Central Java, KnE Engineering, 47-56, 2019. DOI: 10.18502/keg.v4i3.5822

[4] C I Abdullah, N A Magetsari, & H S Purwanto, Analisis dinamik tegasan purba pada satuan batuan Paleogen–Neogen di daerah Pacitan dan sekitarnya,

Provinsi Jawa Timur ditinjau dari studi sesar minor dan kekar tektonik, Bandung: Journal of Mathematical and Fundamental Sciences, 2003, 35(2), pp. 111-127.

[5] M G Rachman, C Prasetyadi, and F Z Adli, Neotectonic Analysis of Magetan-Pacitan Fault Zone, Yogyakarta: AIP Conference Prosiding 2245, 2020. DOI: https://doi.org/10.1063/5.0010291

[6] H Samodra, S Gafoer, and S Tjokrosapoetro, Geological Map of The Pacitan Quadrangel Jawa, Bandung: Geological Research and Development Centre, 1992.

[7] C Hirt et al., New Ultra-High Resolution Picture of Earth's Gravity Field, Geophysical Research Letter, 2013. DOI: https://doi.org/10.1002/grl.50838

[8] M Dentith and S T Mudge, Geophysics for The Mineral Exploration Geoscientist, UK: Cambridge University Press, 2014.

[9] R J Blakely 1996 Potential theory in gravity and magnetic applications, UK: Cambridge University Press, 1996.

[10] M W Telford et al. 1990 Applied Geophysics, UK: Cambridge University Press, 1990.

[11] T Sastranegara, S S Nainggolan, and I B Raharjo, The Application of a Triangular Mesh for Gravity Inversion to Reconstruct Subsurface Geological Structures in the Hululais Geothermal Prospect, Bengkulu, Melbourne: Proceedings World Geothermal Congress, 2015.